Aquatic Toxicology 283 (2025) 107369

Contents lists available at ScienceDirect

Aquatic Toxicology

journal homepage: www.elsevier.com/locate/aqtox

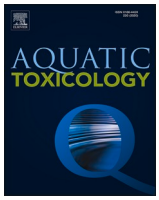

Cellular and tissue-level responses of mussels (*Mytilus edulis*) to aged polyethylene terephthalate (PET) micro- and nanoplastic particles

Jenevieve Hara [a,b,*], Gethrie B. Oraño [a], Maaike Vercauteren [b], Kayawe Valentine Mubiana [a], Colin R. Janssen [b], Ronny Blust [a], Jana Asselman [b], Raewyn M. Town [a]

[a] ECOSPHERE, Department of Biology, University of Antwerp, Groenenborgerlaan 171, Antwerp 2020, Belgium
[b] Blue Growth Research Lab, Ghent University, Wetenschapspark 1, Ostend 8400, Belgium

ARTICLE INFO

Keywords:
Aged micro- and nanoplastics
Polyethylene terephthalate
Environmentally relevant concentrations
Histopathology
Immunotoxicity
Mussels

ABSTRACT

Micro- and nanoplastic particles (MNPs) are pollutants of global concern due to their persistence, ubiquity, and associated risks. Laboratory studies, however, have predominantly focused on pristine MNPs, which do not adequately reflect the characteristics of environmental plastic debris. To address this gap, this study investigated the cellular and tissue-level responses of mussels (*Mytilus edulis*) to aged polyethylene terephthalate (PET) MNPs (diameter 600 nm to 3.1 μm) at three environmentally relevant concentrations: 10, 10^3, and 10^5 particles/L. The particles' physicochemical characteristics and stability in exposure media were analyzed using a combination of advanced analytical techniques. The biological responses were analyzed across multiple effect endpoints during both the exposure (days 1, 3, 7, and 14) and the subsequent recovery periods (3 and 10 days post-exposure), via flow cytometry and histopathology. The results revealed the sensitivity of hemocyte subpopulations, including granulocytes and hyalinocytes, to aged PET MNPs. Concentration- and time-dependent changes in lysosomal stability, oxidative activity, and hemocyte mortality were observed, demonstrating both immediate cellular perturbations and recovery potential to alleviate particle-induced effects. Histopathological analysis of key tissues exhibited significant alterations, particularly in the gill, suggesting potential impairment of essential physiological functions. No mussel mortality or significant changes in growth metrics were observed under the tested experimental conditions. These findings underscore the systemic impacts across multiple tissues of aged MNP exposure and highlight the importance of adopting integrative, environmentally realistic approaches to assess the biological consequences in future research.

1. Introduction

The escalating production and improper disposal of plastic waste have led to the pervasive presence of micro- and nanoplastic particles (MNPs) in aquatic ecosystems. These plastic particles, with defined sizes smaller than 5 mm and 1000 nm, respectively, are now recognized as pollutants of global concern due to their persistence, ubiquity, and associated risks (Khanna et al., 2024). MNPs are introduced into the environment either through direct release or generated via the fragmentation of larger plastic debris. Their size, high surface area-to-volume ratio, and capacity to adsorb harmful chemicals can amplify their potential toxicity, underscoring the urgent need to elucidate the mechanisms underlying the biological effects (da Costa et al., 2019).

Polyethylene terephthalate (PET) is among the most prevalent polymers in marine environments, commonly found in water columns and sediment layers due to its widespread use in consumer products (Ashrafy et al., 2023). Once released into the environment, plastic particles undergo aging processes, including photodegradation, biodegradation, thermal oxidation, and mechanical abrasion. While PET is highly resistant to photodegradation, with photoaging degradation times exceeding 500 years, it can undergo surface modifications through other processes such as hydrolysis and microbial activity (Lu et al., 2023a). For instance, alkali-resistant bacteria have been shown to degrade PET microplastics, causing 11.04 % weight loss and visible etching and fractures on the PET fiber surface within five days (Li et al., 2023). These processes not only modify the surface properties of particles but also influence their environmental behavior, including their tendency to aggregate, position within the water column, and accumulation in sedimentary environments (Galloway et al., 2017). Such changes

* Corresponding author at: ECOSPHERE, Department of Biology, University of Antwerp, Groenenborgerlaan 171, Antwerp 2020, Belgium
E-mail address: jenevieve.hara@uantwerpen.be (J. Hara).

https://doi.org/10.1016/j.aquatox.2025.107369
Received 21 January 2025; Received in revised form 31 March 2025; Accepted 13 April 2025
Available online 15 April 2025

increase the risks posed to benthic habitats and organisms, particularly filter feeders, which are directly exposed to these particles in both the water column and sediment layers.

Benthic organisms, such as mussels, are particularly susceptible to ingesting plastic particles (Canesi et al., 2012). Mussels are widely used as sentinel organisms for monitoring marine pollution due to their wide geographic distribution, ecological significance, and feeding behavior (Beyer et al., 2017). As filter feeders, mussels process large volumes of water, making them prone to ingesting suspended MNPs, which can subsequently accumulate in their tissues and translocate to the circulatory system (Canesi et al., 2012; Ribeiro et al., 2019). These traits, combined with their ease of cultivation for aquaculture, and their established role as bioindicators (Beyer et al., 2017), mark their significance as both a model organism and proxy for assessing the risks associated with MNP exposure.

Previous studies have extensively examined the effects of MNPs, documenting diverse biological responses, including oxidative stress, immune dysfunction, histopathological alterations, and other physiological changes (Barría et al., 2025). A meta-analysis focused on bivalves identified oxidative stress as a key mechanism of MNP toxicity, characterized by a time-dependent induction that disrupts redox balance and leads to cellular damage (Li et al., 2022). However, the environmental relevance of such studies remains limited, as they predominantly focus on pristine, commercially available particles, while aged plastics, which exhibit altered physicochemical properties, have received comparatively less attention (Cunningham et al., 2023). Accurately simulating environmentally realistic exposure scenarios requires test particles that mirror those found in natural environments, accounting for particle aging, polymer type, shape, concentration, and size ranges (Revel et al., 2021). Despite advances in understanding the toxicity of pristine MNPs, most laboratory studies employ concentrations orders of magnitude higher than those found in natural environments (Lenz et al., 2016). Additionally, PET, one of the most commonly detected MNP polymers in mussels, remains underrepresented in toxicity studies (Barría et al., 2025; Fraissinet et al., 2024). Particularly, particles in the nano-sized range pose heightened risks due to their ability to bioaccumulate, cross biological barriers, penetrate cells, and influence cellular and tissue systems (Browne et al., 2008; Fernández and Albentosa, 2019b, 2019a).

Assessing immunological and histopathological endpoints can provide critical insights into the cellular and tissue-level responses induced by aged particles (Hara et al., 2024). In mussels, hemocyte-mediated immune responses, including lysosomal stability, oxidative activity, and cellular mortality, serve as key indicators of particle-induced toxicity. Disruptions to these immune functions can compromise homeostasis and trigger systemic stress responses (Canesi and Procházková, 2014). Given the persistence and aging processes of MNPs in natural environments, their capacity to induce immune dysfunction may be exacerbated by co-occurring stressors, further compromising physiological and defense performance in mussels (Huang et al., 2022; Mkuye et al., 2022). Similarly, histopathological alterations in key tissues, such as the gills and digestive gland, offer valuable indicators of morphological and structural changes associated with physiological dysfunction. In the digestive gland, endpoints such as lipofuscin aggregation, hemocyte infiltration, atrophy, and necrosis, are indicative of inflammatory response and regressive and progressive changes in tissue structure (Bouallegui et al., 2018; Carella et al., 2015). Additionally, histopathological changes in the gills, particularly lamellar fusion, and the enlargement of the central vessel, can significantly impair essential functions, including filtration, respiration, osmoregulation, and particle transport (Leis et al., 2024). Integrating these multiple histopathological alterations into condition indices provides a robust framework for linking sensitivity to particle exposure effects with tissue integrity and organismal health (Costa et al., 2013). Collectively, these endpoints can reveal the systemic impacts of MNP exposure and offer an integrative approach to understanding their broader biological consequences.

In this study, we tested the hypothesis that aged PET MNPs, exhibiting environmentally relevant particle characteristics, elicit pronounced and potentially persistent adverse effects at both cellular and tissue levels. Specifically, we aimed to mechanistically evaluate the immunological and histopathological responses of blue mussels (*Mytilus edulis*) following in vivo exposure to aged PET MNPs under environmentally relevant conditions. A suite of cellular and tissue-level endpoints was assessed at multiple timepoints during both the exposure (days 1, 3, 7, and 14) and recovery (3 and 10 days post-exposure) periods to capture the dynamics of biological responses.

2. Materials and methods

2.1. Characterization of the aged PET micro- and nanoplastic particles

The stock suspension of chemically aged polyethylene terephthalate (PET) micro- and nanoplastic particles (MNPs) was prepared and provided by the European Commission Joint Research Centre (JRC in Geel, Belgium), with detailed procedures reported in Seghers et al. (2025). Aged PET particles were suspended in Milli-Q water without surfactant. The particles had an average dimension, D, of 1.9 μm, with size distribution values of D_{10} = 600 nm, D_{50} = 1.4 μm, and D_{90} = 3.1 μm, as analyzed using the Single Particle Extinction and Scattering (SPES) technique (ClassizerONE S1.4.34, EOS; JRC in Ispra, Italy). D_{10}, D_{50}, and D_{90} denote the particle sizes below which 10 %, 50 %, and 90 % of the total population fall, respectively. This size range is ecologically relevant, as it encompasses the predominant plastic particle sizes accumulating in mussel hemolymph (Browne et al., 2008) and key tissues, including the digestive gland and gills (Fernández and Albentosa, 2019a). The primary stock solution used in this study contained 4.0×10^7 particles/mL.

The aged PET MNPs were verified with a 0.97 match score to the reference spectrum using Raman spectroscopy and Open Specy reference library. Complementary scanning electron microscopy (SEM, Phenom™ ProX) images confirmed the fragmented and irregular shapes of particles (Supplementary Fig. A.1, Panel A, B, and C). To ensure particle stability under in-vivo exposure conditions, the hydrodynamic size, zeta-potential, and electrophoretic mobility of aged PET MNPs in filtered artificial seawater (100 nm membrane filters, Millipore) was measured at 1 h, 24 h, and 48 h using Dynamic Light Scattering (DLS, Zetasizer Nanoseries, Malvern Instruments). Prior to analysis, the surfactant-free stock suspension of aged PET MNPs was sonicated for 20 min, and a working solution (10^5 particles/mL) was prepared in sterile glass containers using filtered ASW. Reference standards (ZTS1240, Malvern Panalytical) were included for quality control, and three replicate measurements in folded capillary cell were performed per time point. Specifically, the electrophoretic mobility was measured at a constant direct current electric field of 10 V/cm. The particles displayed relatively uniform dispersion over time, with hydrodynamic diameters ranging from 478 nm to 650 nm. Zeta potential measurements illustrated particle stability in ASW, with values remaining between –14.7 mV and –17.1 mV, aligning with electrophoretic mobility data (–1.04 to –1.21 μm·cm/V·s) (Supplementary Fig. A.2).

2.2. Test organisms

Approximately 400 adult blue mussels (*Mytilus edulis*) with a mean shell length of 43.4 ± 2.47 mm and wet weight of 15.2 ± 2.54 g were collected from Hoedekenskerke, The Netherlands. Mussels were kept in glass aquaria with artificial seawater (ASW) prepared using purified water from double-pass reverse osmosis (RO) units (Eurowater) and high-quality sea salt (hw-Marinemix Professional). The tanks were equipped with portable aeration (Eheim Air Pump 400) and mechanical-biological filtration (Eheim Biopower 200) systems. The temperature was maintained at 15 ± 0.5 °C with 12:12 h photoperiod. Mussels were fed every two days with microalgae suspension (*Tetraselmis suecica*,

Tetraprime S Proviron), at a final concentration of 4–5 × 10^6 cells per mussel (equivalent to 4000–5000 cells/mL), supporting optimal filtration efficiency and growth (Li et al., 2020; Riisgard, 1991; Riisgard et al., 2011) and in line with feeding regimes used in other toxicity studies of comparable or extended duration (Bråte et al., 2018; Pinto et al., 2019; Santana et al., 2018). Water inflow was interrupted for 2 h during feeding. Water was renewed daily by 50 %, and quality parameters (pH: 8.10 ± 0.04, salinity: 31.2 ± 0.4 ‰, dissolved oxygen: 8.15 ± 0.10 mg/L, ammonia: 0.25 mg/L, nitrite: <0.3 mg/L, and nitrate: 12.5 mg/L) were monitored using Hach HQ40D meters and Tetra test kits (Von Moos et al., 2012). Mussels were acclimated and depurated for at least three weeks, with no mortality observed during this period.

2.3. Experimental set-up

In total, 12 aquaria were set up for the in vivo experiment, each containing 30 individuals (1 L ASW per individual). A negative control (NC) group in triplicate was maintained in clean ASW throughout the experiment. Exposure treatments comprised three nominal concentrations of aged PET MNPs: 10 particles/L (C1), 10^3 particles/L (C2), and 10^5 particles/L (C3). These concentrations align with modeled scenarios for marine environments (Besseling et al., 2019; Lenz et al., 2016) and reflect the estimated exposure concentrations assuming the complete degradation of spherical PET particles (Sioen et al., 2024).

Each experimental condition included three replicate aquaria, all maintained under the same controlled conditions as described above. Mussels were randomly placed in glass petri dishes in groups of five, corresponding to the number of individuals collected at each timepoint. This setup facilitated byssal attachment and minimized handling stress during water renewal (as illustrated in Supplementary Fig. A.3). Exposure was conducted continuously for 14 days, during which mussels were fed every two days as previously described (Section 2.2). After each feeding, the water was completely renewed and replenished with the appropriate volume of aged PET MNPs from the working suspension (10^6 particles/mL) to maintain target exposure concentrations, based on water volume and mussel count (Supplementary Table A.1). The particle stock suspension was sonicated for 20 min before use.

During the exposure period, five mussels (thus one glass petri dish) per tank were collected at four time points (D1, D3, D7, D14) for analysis. The 14-day exposure period was followed by a 10-day recovery period, chosen based on the observed timeline for plastic particle uptake and elimination (Fernández and Albentosa, 2019b). For this, the remaining mussels from aged PET MNP treatment tanks were rinsed with ASW and transferred to clean tanks for recovery. After 3 and 10 days post-exposure, samples were again collected.

Throughout the experiment, each tank was aerated using two glass pipettes connected to a silicone hose for constant aeration and to promote uniform particle dispersion. Tanks were covered with aluminum foil to prevent contamination.

2.4. Sampling procedure

Mussel condition was assessed individually at baseline (day 0) and each timepoint by measuring shell length (mm) with a digital caliper (0.1 mm precision) and weight (g) with a scale (0.01 g precision). At each time point, five mussels (thus one glass petri dish) were collected from each replicate aquarium (15 individuals per experimental condition), and then anesthetized for 30 min in a filtered (100 nm, Millipore) and sterilized 0.3 M magnesium chloride ($MgCl_2$) solution. Hemolymph was extracted from the posterior adductor muscle using a sterile 2 mL syringe (Injekt) with a 23 G needle (Terumo Neolus), pooled, and then filtered through a 70 µm cell strainer (Greiner) (Auguste et al., 2020; Canesi et al., 2015). Samples were maintained at 4 °C in a final volume of 300 µL per assay to minimize hemocyte aggregation until further analysis (Chen and Bayne, 1995) (Section 2.5.1–2.5.3). For histopathological examination, the digestive gland and gill tissues were dissected from 2 mussels per replicate aquarium using a sterile kit. Tissues were fixed overnight in 4 % paraformaldehyde (PFA, Invitrogen) at 4 °C, and rinsed three times in phosphate-buffered saline (PBS, 0.01 M). Samples were stored at 4 °C until analysis (Section 2.6.1). All procedures were conducted in a laminar flow cabinet (Spetec).

2.5. Assessment of cellular-level effect endpoints

The responses of hemocyte subpopulations to aged PET MNPs were analyzed by fluorescent labeling and flow cytometry with BD™ LSR II (BD Biosciences), as previously applied (Hara et al., 2024; Wang et al., 2019).

2.5.1. Lysosomal stability

Lysosomal stability was assessed using the LysoTracker™ Blue DND-22 (Invitrogen). Hemolymph samples (300 µl) were incubated with LysoTracker to a final concentration of 75 nM and incubated in the dark at 15 °C for 1 h. Fluorescence was measured with excitation and emission wavelengths of 373 nm and 422 nm, respectively. Data were expressed as the mean geometric fluorescence in hemocyte subpopulations relative to the negative control (set to 100 %).

2.5.2. Reactive oxygen species (ROS) production

The intracellular reactive oxygen species (ROS) levels were evaluated using the 5-(and-6)-chloromethyl-2′,7′-dichlorodihydrofluorescein diacetate acetyl ester (CM-H2DCFDA, Invitrogen), dissolved in dimethylsulfoxide (DMSO). To validate assay sensitivity, oxidative activity was induced with 100 µM H_2O_2 as a positive control (Hara et al., 2024; Sendra et al., 2020). Hemolymph samples (300 µl) were incubated with CM-H_2DCFDA to a final concentration of 10 µM and incubated in the dark at 15 °C for 1 h. Fluorescence was measured with the FITC signal detector of the flow cytometer. Data were expressed as the mean geometric fluorescence in hemocyte subpopulations relative to the negative control (set to 100 %).

2.5.3. Hemocyte mortality

Hemocyte mortality was assessed using Propidium Iodide (PI; Abcam), following the manufacturer's protocol with modification (Wang et al., 2019). As previously reported (Hara et al., 2024; Olabarrieta et al., 2001), cadmium chloride ($CdCl_2$, 800 µM) was used as a chemical control (PC CT), while 1-h sonication served as a non-chemical control (PC ST) to induce cell death. Hemolymph samples (300 µl) were incubated with 5 µl of PI, and incubated in the dark at 15 °C for 5–10 min. Fluorescence was measured with excitation and emission wavelengths of 535 nm and 617 nm, respectively. Data were expressed as the percentage (%) of cells with iodide fluorescence relative to the total number in each hemocyte subpopulation.

2.5.4. Flow cytometry analyses

All measurements were performed with BD LSR II flow cytometer (BD Biosciences) equipped with 488 nm (blue), 633 nm (red), 405 nm (violet), and 355 nm (UV) lasers. Hemocyte subpopulations were detected based on side scatter (SSC) and forward scatter (FSC) parameters, which reflect cell size and internal complexity, respectively. A total of 10,000 cells were analyzed for each sample replicate. To ensure accurate parameter measurements throughout the experiment, regular calibration was conducted using calibration beads. Data were processed using FACSDiva™ Software (Version 5.0) and FlowJo (Version 10.9.0).

2.6. Assessment of tissue-level effect endpoints

The effect of aged PET MNP exposure on mussel physiology was assessed through histopathological examination of tissues.

2.6.1. Histopathological analysis

Digestive gland and gill tissues were collected from two mussels per replicate aquarium (six mussels in total) from the control and the highest-aged PET treatment (C3) groups at the end of the exposure (day 14) and recovery period (10 days post-exposure). Samples were processed for histopathological analysis at the Antwerp Centre for Advanced Microscopy (ACAM). Fixed tissues were dehydrated through a series of graded ethanol, cleared in xylene, and then embedded in paraffin. Tissue samples were sectioned at 5 μm using a microtome, then stained with hematoxylin and eosin (H&E) (Costa et al., 2013). The stained sections were fully scanned using a Zeiss Axioscan digital slide scanner. Six tissue sections of the digestive gland and gills, each with eight image annotations, were analyzed per treatment (48 in total) using QuPath software (Version 0.4.3).

2.6.2. Histopathological condition indices

The semi-quantitative histopathological condition index (I_h) was calculated for gills and digestive glands of mussels by following the method previously employed (Costa et al., 2013; Ertürk Gürkan and Gürkan, 2021; Pinto et al., 2019). The I_h was calculated based on the differential biological significance of each observed alteration (weight) and its degree of dissemination (score). The weights (w) assigned to each histopathological alteration (j), as described by Ertürk Gürkan & Gürkan (2021) were applied to assess changes in the digestive gland (lipofuscin aggregation, hemocyte infiltration, hyperplasia, atrophy, and necrosis) and gills (lipofuscin aggregation, hemocyte infiltration, enlarged central vessel, loss of cilia, and lamellar fusion). The weight ranged from 1 (indicating minimum severity) to 3 (maximum severity), and the score ranged from 0 (alteration not observed) to 6 (diffuse). I_h was calculated using the described formula:

$$I_h = \frac{\sum_i^j w_j a_{jh}}{\sum_i^j M_j}$$

where I_h is the histopathological condition index calculated per organ for each individual mussel h; w_j the weight of the jth histopathological alteration; a_{jh} the score attributed to the hth individual for the jth alteration; and M_j is the maximum attributable value (weight × maximum score) for the jth alteration. The equation denominator normalizes I_h to a value between 0 and 1.

The I_h results were then categorized based on the prevalence of histopathological alterations as follows: low (0–0.25), moderate (0.25–0.50), high (0.50–0.75), or very high (0.75–1) (Costa et al., 2013).

2.7. Statistical analysis

The data were assessed for normality using Shapiro-Wilk test. Statistical analyses were then performed to assess the significant effects of exposure concentration and time using either one-way analysis of variance (ANOVA) or the non-parametric Kruskal-Wallis, followed by Tukey's HSD or Dunn's post-hoc test, respectively. The intensities of histopathological conditions (semi-quantitative data) were compared using the Mann-Whitney U test to assess differences between control and exposed groups across exposure and depuration periods. Statistical significance was set at $P < 0.05$. All analyses were performed using GraphPad Prism (Version 10.1.2). The graphical abstract was created in BioRender (Hara, 2025): https://BioRender.com/lzxe4xy.

2.8. Quality assurance and control

This experiment achieved a score of 62.5 % (25/40) on the proposed quality assurance and control (QA/QC) criteria, surpassing the reported average score of 44.6 % (De Ruijter et al., 2020). Although using MNPs posed analytical challenges that hindered compliance with quality criteria 8, 9, and 11 for background contamination, exposure concentration, and organism exposure (e.g., MNP ingestion or accumulation), the overall score demonstrates strong quality performance. Detailed explanations for each criterion are provided in Supplementary Table A.2.

3. Results

3.1. Cellular responses to aged PET MNP exposure

The responses of mussels to exposure with varying concentrations of aged PET MNPs (10 (C1), 10^3 (C2), and 10^5 (C3) particles/L) were assessed across multiple cellular effect endpoints during both the exposure (days 1, 3, 7, and 14) and recovery periods (days 17 and 24 or 3 and 10 days post-exposure), respectively.

3.1.1. Lysosomal content stability

Lysosomal content in granulocytes (Fig. 1, panel A) showed relative fluctuations over time, although no statistically significant differences were observed across all tested aged PET concentrations and the negative control during both the exposure and recovery periods. In contrast, hyalinocytes (Fig. 1, panel B) exhibited a significant decrease in lysosomal content only at the highest aged PET MNP concentration (C3) compared with the control after 3 days of exposure ($p = 0.016$). No significant changes, indicating lysosomal content recovery, were

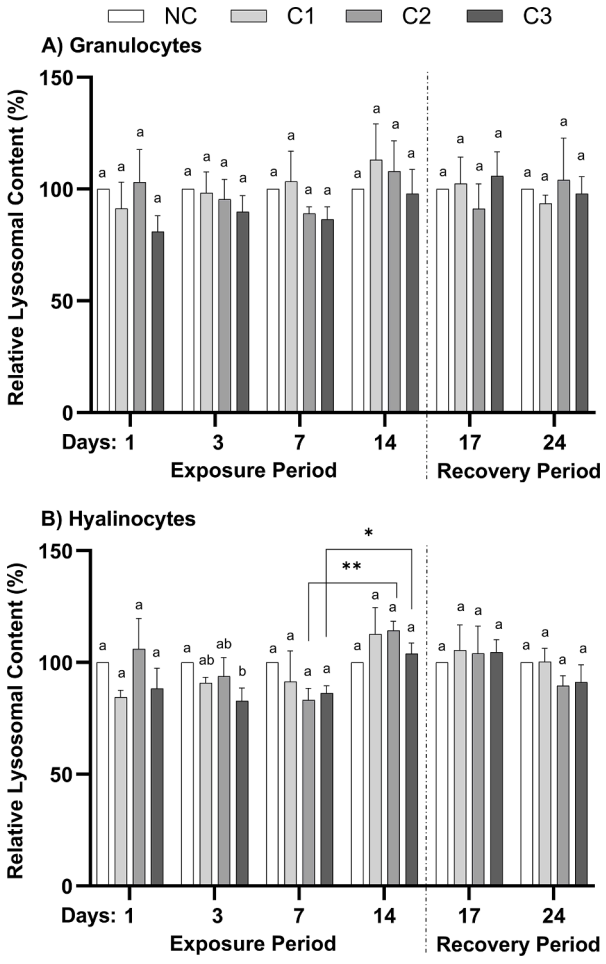

Fig. 1. Relative lysosomal content in (A) granulocytes and (B) hyalinocytes exposed to different concentrations of aged PET (10 (C1), 10^3 (C2), and 10^5 (C3) particles/L) over the exposure (Days 1, 3, 7, and 14) and depuration periods (3 and 10 days post-exposure). Data are expressed as mean ± SD ($n = 3$). Different lower-case letters denote significant differences among concentrations at each time point ($P < 0.05$), while asterisks indicate significant differences within each concentration over time (*$P < 0.05$; **$P \leq 0.01$; ***$P \leq 0.001$).

observed by day 7 and maintained throughout the subsequent exposure and recovery periods.

3.1.2. Oxidative activity

In granulocytes (Fig. 2, Panel A), exposure to the lowest concentration of aged PET (C1) did not induce significant changes in ROS levels throughout both the exposure and recovery periods. However, exposure to aged PET MNP C2 induced a significant decrease in ROS levels only on day 14 of the exposure period ($p = 0.023$), while C3 exhibited a significant decrease 3 days post-exposure compared to the control ($p = 0.012$) and lower concentrations (C1: $p = 0.029$ and C2: $p = 0.003$). Similarly, in hyalinocytes (Fig. 2, Panel B), aged PET MNP C2 exposure led to a significant decrease in ROS levels only on day 14 compared to the control ($p = 0.049$). Although C3 resulted in the lowest ROS levels three days post-exposure, this difference was not statistically significant from the concurrent control. The observed changes in both granulocytes and hyalinocytes were transient, with no significant changes in ROS levels compared to the control by 10 days post-exposure, demonstrating reversibility.

3.1.3. Hemocyte mortality

As shown in Fig. 3 (Panel A), exposure to aged PET C2 ($p = 0.006$) and C3 ($p < 0.0001$) significantly increased mortality in granulocytes only after 3 days of exposure while C1 ($p = 0.021$) induced an increase only after 7 days of exposure compared with the control. No significant increases in granulocyte mortality were observed by day 14 compared with the concurrent control and maintained throughout the subsequent recovery period.

In hyalinocytes (Fig. 3, Panel B), only the aged PET C3 ($p = 0.001$) induced a significant increase in mortality compared with the control after 3 days of exposure. Subsequently, by day 7, the C2 treatment group displayed the lowest percentage of hemocyte mortality among all treatments ($p < 0.05$). Similar to granulocytes, no significant changes in hyalinocyte mortality were observed compared with the control by day 14 of the exposure period and throughout the recovery period.

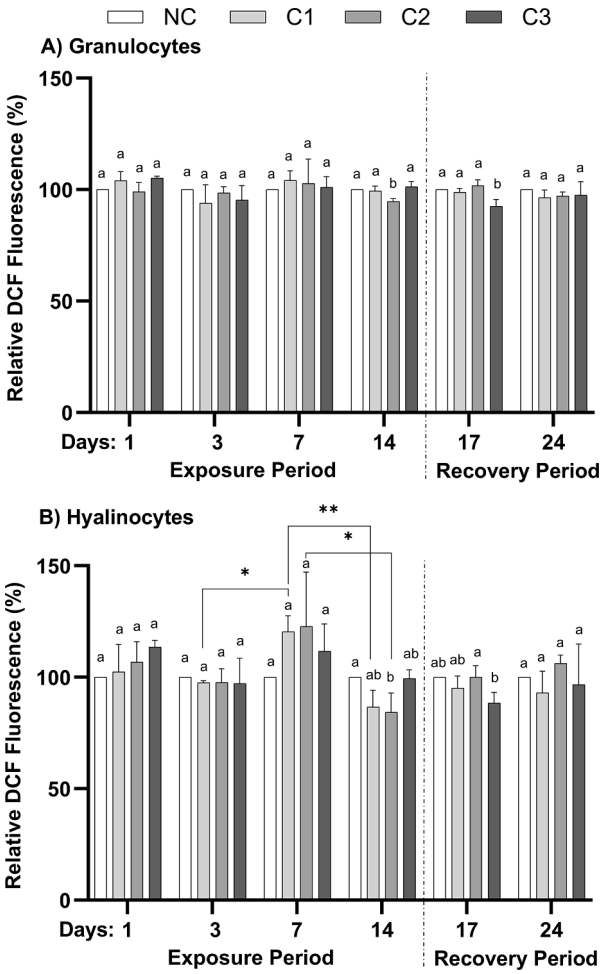

Fig. 2. Relative reactive oxygen species (ROS) production in (A) granulocytes and (B) hyalinocytes exposed to different concentrations of aged PET (10 (C1), 10^3 (C2), and 10^5 (C3) particles/L) over the exposure (Days 1, 3, 7, and 14) and depuration periods (3 and 10 days post-exposure). Data are expressed as mean ± SD ($n = 3$). Different lower-case letters denote significant differences among concentrations at each time point ($P < 0.05$), while asterisks indicate significant differences within each concentration over time (*$P < 0.05$; **$P \leq 0.01$; ***$P \leq 0.001$).

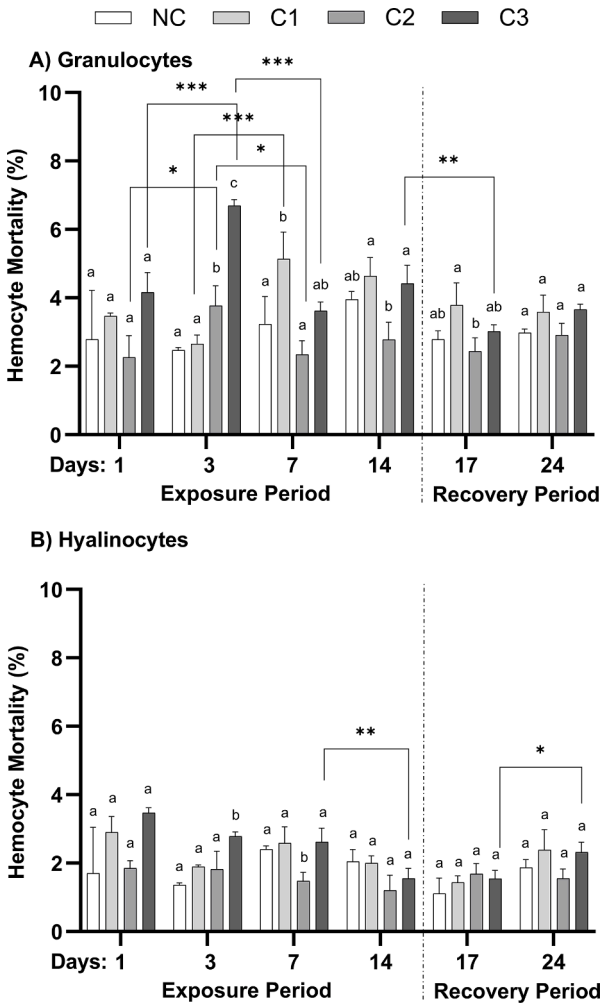

Fig. 3. Hemocyte mortality in (A) granulocytes and (B) hyalinocytes exposed to different concentrations of aged PET (10 (C1), 10^3 (C2), and 10^5 (C3) particles/L) over the exposure (Days 1, 3, 7, and 14) and depuration periods (3 and 10 days post-exposure). Data are expressed as mean ± SD ($n = 3$). Different lower-case letters denote significant differences among concentrations at each time point ($P < 0.05$), while asterisks indicate significant differences within each concentration over time (*$P < 0.05$; **$P \leq 0.01$; ***$P \leq 0.001$).

3.2. Histopathological responses to aged PET MNP exposure

The histopathological responses and condition indices of the digestive gland and gills were assessed during both the exposure (day 14) and recovery periods (10 days post-exposure) (Figs. 4–6).

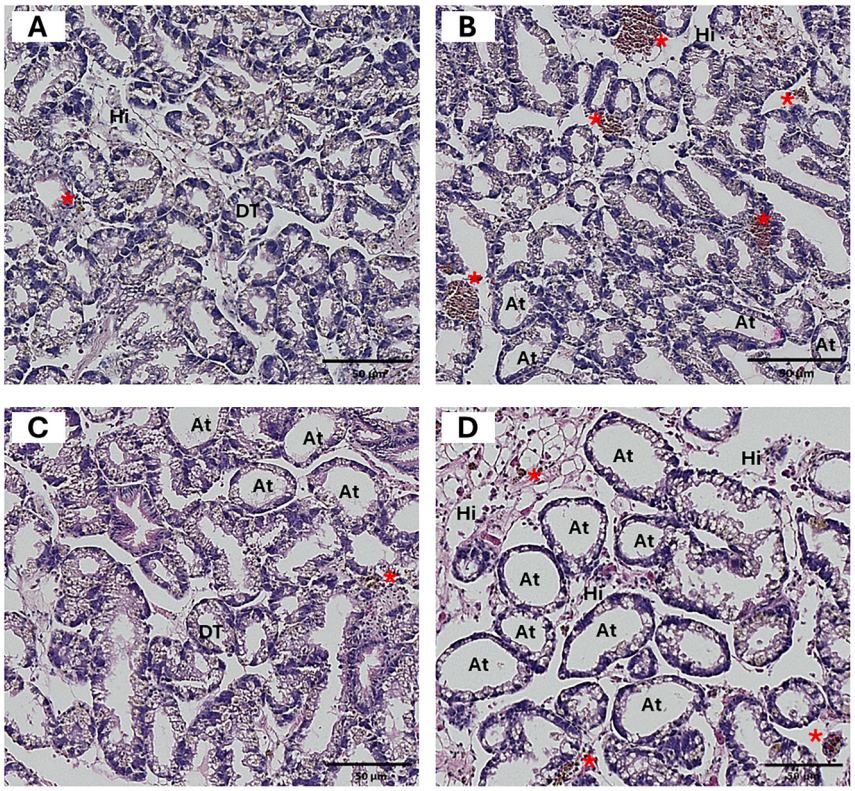

Fig. 4. Micrographs of the digestive gland of *M. edulis* in (A, C) control and (B, D) exposed groups following a 14-day exposure to aged PET (C3: 10^5 particles/L) and a subsequent 10-day recovery period, respectively. **A.** Digestive tubules in the control group showing normal structure (DT) constituted by a single layer of cells surrounding a narrow or occluded tubular lumen with minimal presence of hemocyte infiltration (Hi) and lipofuscin aggregation (red asterisks). **B.** Section of the digestive gland from the exposed group after a 14-day exposure period to aged PET (C3) displaying atrophied digestive tubules (At) with enlarged lumen, thinner epithelium, and pronounced lipofuscin aggregation (red asterisks) characterized by brown pigments. **C.** Section from the control group following the 10-day recovery period showing minimal occurrences of the atrophied tubules (At) and lipofuscin aggregations (red asterisks). **D.** The exposed group following the recovery period with more pronounced occurrences of atrophied digestive tubules (At), hemocyte infiltrations (Hi), and lipofuscin aggregations (red asterisks). Scale bar: 50 μm.

3.2.1. *Digestive gland*

As shown in Fig. 4, the digestive gland for control samples demonstrated normal structure, with digestive tubules characterized by a single layer of cells surrounding a narrow or occluded tubular lumen. In comparison with the control, the group exposed to the highest concentration of aged PET (C3) exhibited pronounced occurrences of atrophic and necrotic digestive tubules, particularly during the depuration period. The exposed groups also exhibited a higher extent of hemocyte infiltration and larger lipofuscin aggregation. Although the exposed group exhibited a relatively higher I_h (Fig. 6, Panel A) compared to the control group during both the exposure ($p = 0.316$) and recovery periods ($p = 0.080$), these differences were not statistically significant. The I_h remained consistently within the low category (0 – 0.25), across both the control (NC) and exposed groups (C3).

3.2.2. *Gills*

The histopathological analysis of the gill filaments (Fig. 5) in control samples demonstrated the typical structure, with well-defined lamellae formed by a single layer of epithelial cells, tightly structured central vessel, and minimal presence of lipofuscin aggregation and hemocyte infiltration. In contrast, exposure to the highest tested concentration of aged PET (C3) induced several lesions in the gill tissues. These changes included a progressive presence of lamellar fusion in the lateral and abfrontal zones coupled with the enlargement of the central vessels, particularly evident during the exposure period. A higher extent of hemocyte infiltrations and lipofuscin aggregations were observed in association with gill filaments showing regressive changes. The I_h for gills (Fig. 6, Panel B) was significantly higher in the exposed group (aged PET C3) compared to the control during the exposure period ($p = 0.004$). By the recovery period, the I_h in the exposed group (C3) remained significantly elevated ($p = 0.015$), with an index value within the moderate category (0.25 – 0.50), compared to the control (low, 0 – 0.25).

3.3. *Growth and survival of mussels exposed to aged PET MNPs*

Exposure to aged PET MNPs did not result in mortality or significant alterations in growth parameters, including weight and shell length, in mussels (Supplementary Fig. A.4, Panels A and B). The mean shell length (41.7–46.3 mm) and mean weight (13.8–17.1 g) remained consistent across all groups during both the exposure period and recovery period. Statistical analysis of absolute changes, calculated as the difference between baseline (Day 0) and final values, confirmed no significant differences ($p > 0.05$) in these parameters across the negative control (NC) and treatment groups exposed to varying concentrations of aged PET MNPs.

4. Discussion

This study provides an integrative analysis of cellular, tissue, and organismal-level responses of mussels exposed to environmentally relevant concentrations of aged PET MNPs. Current findings reveal concentration- and time-dependent effects, demonstrating both immediate cellular perturbations and recovery potential. Histopathological analysis revealed tissue-specific alterations. While no immediate effects on growth and mortality were observed in mussels, long-term implications for organismal health cannot be excluded nor potential mixture effects with other stressors.

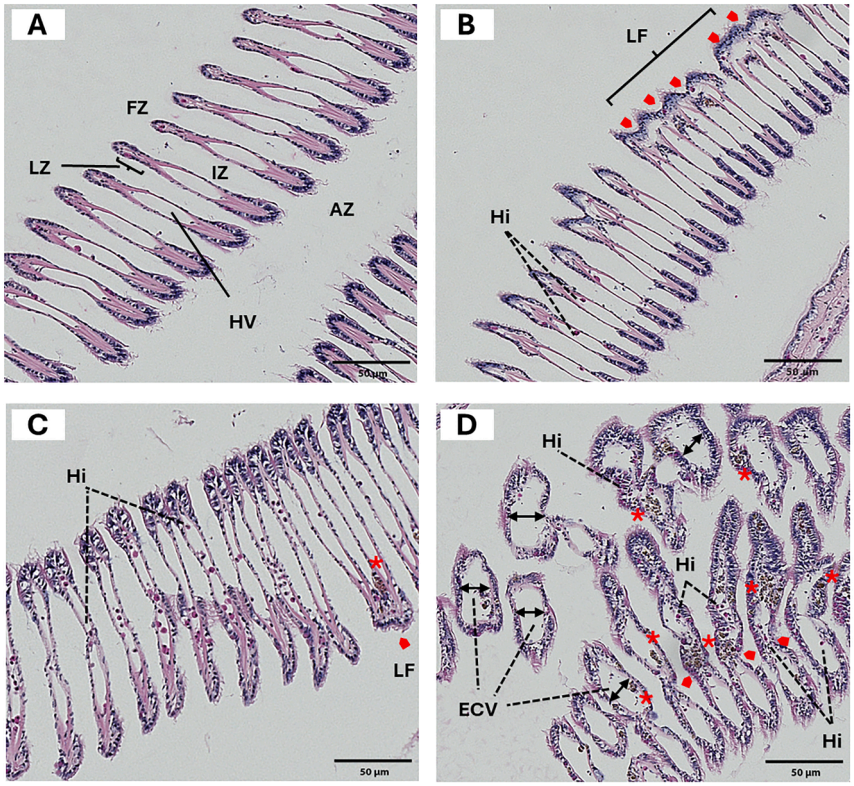

Fig. 5. Micrographs of the longitudinal section through the gill filaments of *M. edulis* in (A, C) control and (B, D) exposed groups following a 14-day exposure to aged PET (C3: 10^5 particles/L) and a subsequent 10-day recovery period, respectively. **A.** Gill filaments in the control group showing normal structure with indication of the frontal zone (FZ), lateral zone (LZ), abfrontal zone (AZ), intermediate zone (IZ), and hemolymphatic vessel (HV). **B.** Gill filaments in the exposed group following a 14-day exposure period to aged PET (C3) exhibiting lamellar fusion (LF, red arrowheads) in the lateral zone **C.** Control group following the 10-day recovery period with indications of lipofuscin aggregations (red asterisks) and hemocyte infiltrations (HI). **D.** The exposed group following the recovery period with an evident enlargement of the central vessel (ECV, double-headed arrows), lamellar fusion in the abfrontal zone (LF, red arrowheads), including abundant lipofuscin aggregations (red asterisks) and hemocyte infiltrations (HI). Scale bar: 50 µm.

4.1. Cellular responses to aged PET MNP exposure

In marine bivalves, hemocytes are multifunctional circulating cells essential for immune defense, nutrient transport, tissue repair, and maintaining homeostasis (de la Ballina et al., 2022). Understanding the responses of hemocyte subpopulations, such as granulocytes and hyalinocytes, to aged plastic particle exposure is crucial for assessing impacts on immune function and physiological resilience.

Cellular responses, such as perturbations in lysosomal integrity and stability, are regarded as sensitive indicators of cellular injury (Moore et al., 2006). In the current study, granulocytes demonstrated resilience to aged PET MNP exposure, maintaining lysosomal stability even at the highest tested concentration. In contrast, hyalinocytes exhibited significant lysosomal destabilization only at the highest concentration (C3) after 3 days of exposure. These results are in line with those obtained for undifferentiated mussel hemocytes (*Mytilus galloprovincialis)*, where a significant decrease in lysosomal membrane stability (LMS) was observed after 21 days of exposure to 50 nm PS-NPs (1.5–150 ng/L or 2.17×10^5–2.17×10^7 particles/L) and 3 µm PS MPs (15–150 ng/L; 1000–10,000 particles/L), as measured by the NRRT assay (Capolupo et al., 2021). Another study performed at higher particle concentrations reported prominent lysosomal destabilization induced by amino polystyrene NPs (50 nm PS-NH_2, 10 µg/L or 1.46×10^{11} particles/L converted concentrations in Supplementary Table A.3) after 24 h of exposure, and, to a lesser extent upon repeated exposure following 3 days of depuration (Auguste et al., 2020). This transient destabilization contrasts with nano titanium dioxide (TiO_2, 25 and 100 nm at 0.1–10 mg/L or 2.89×10^{12}– 2.89×10^{14} and 4.52×10^{10}–4.52×10^{12} particles/L, respectively), which induced concentration- and size-dependent lysosomal destabilization in mussels that persists throughout both exposure and recovery periods (Wang et al., 2019).

ROS are naturally produced in all cells, including hemocytes, but overproduction can lead to oxidative damage and disrupt homeostasis (Li et al., 2022). As observed, exposure to moderate (C2) and high (C3) concentrations of aged PET caused a significant but transient reduction in ROS levels in both hemocyte subpopulations. Similarly, a transient ROS reduction in oyster hemocytes (*Crassostrea hongkongensis*) was observed after 7-day *in-vivo* exposure to zinc (Zn, 300 µg/L, 4.6×10^{-6} M), primarily in granulocytes and to a lesser extent in hyalinocytes, with no significant changes at subsequent time points (Luo and Wang, 2022). These findings are notable because they diverge from the typically observed oxidative stress response—where MNP exposure has been linked to increased ROS production in various cell types (Hu and Palić, 2020). Recent findings suggest that physicochemical changes associated with plastic aging can modulate ROS dynamics. Specifically, Jeon et al. (2021) demonstrated that weathered plastic particles, despite higher intrinsic ROS potential, generated less ROS in biological media due to enhanced protein binding, leading to lower net ROS levels in cellular systems. Although our study did not directly assess antioxidant responses, the ROS reduction observed may also reflect a compensatory activation of endogenous antioxidant systems. Key enzymes such as catalase (CAT), superoxide dismutase (SOD), glutathione peroxidase (GPx), and glutathione (GSH) can be upregulated in response to particle-induced oxidative stimuli (Li et al., 2022). For instance, mussel (*Mytilus spp*.) exposed to mixed PS MPs (2–6 µm, 32 µg/L or 2.0×10^6 particles/L) combined with fluoranthene (30 µg/L or 1.5×10^{-7} M)

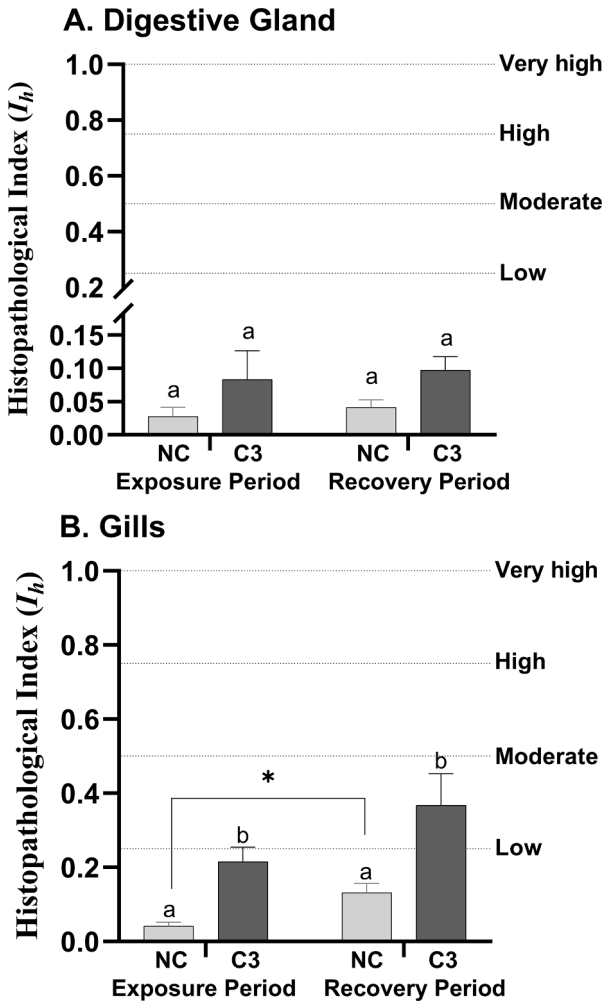

Fig. 6. Histopathological condition indices (I_h) in the (A) digestive gland and (B) gills of *M. edulis* for control (NC) and exposed groups (aged PET C3: 10^5 particles/L) after the exposure period (Day 14) and recovery period (Day 24; 10 days post-exposure). Data are expressed as mean ± SE ($n = 6$ tissue replicates per treatment). The I_h were categorized according to Costa et al. (2013) as low (0–0.25), moderate (0.25–0.50), high (0.50–0.75), or very high (0.75–1). Different lower-case letters denote significant differences between the groups within each period, while asterisks indicate significant differences within each group over time (Mann-Whitney U, $P < 0.05$).

efficiently neutralized ROS, linked to antioxidant activation and low lipid peroxidation (Paul-Pont et al., 2016). The transient nature of ROS reductions suggests that aged PET MNPs, like other chemicals, can temporarily alter cellular redox balance, potentially contributing to cumulative mixture effects.

Consequently, the current findings, in combination with previous in vitro studies on aged PET MNPs (Hara et al., 2024), reveal significant concentration- and time-dependent effects on hemocyte mortality. As observed, granulocytes showed early susceptibility, with increased mortality observed after 3 days of exposure to aged PET C2 and C3, while C1-induced effects were delayed until day 7. In contrast, hyalinocytes exhibited significant changes in mortality only when exposed to aged PET C3 after 3 days of exposure. Similarly, exposure to environmental polyethylene (PE) NPs (1–1200 nm, 0.08 μg/L or 9.61×10^4–1.66×10^{14} particles/L) and MPs (1.2–300 μm, 0.08 and 10 μg/L, or within 6.15×10^{-3}–1.20×10^7 particles/L, calculated based on the given mass concentration and the full range of particle sizes) induced concentration-dependent cytotoxicity, reducing cell viability within 24 h (Roman et al., 2023). In comparison, metallic nanoparticles such as TiO_2 (25 and 100 nm at 0.1–10 mg/L or 2.89×10^{12}–2.89×10^{14} and 4.52×10^{10}–4.52×10^{12} particles/L, respectively) induce sustained hemocyte mortality even after 14 days post-exposure, which was attributed to the synergistic interplay of particle size and concentration (Wang et al., 2019).

The differential sensitivity of granulocytes and hyalinocytes to aged PET particles likely reflects their distinct immune functions. Granulocytes, characterized by high phagocytic activity, are more actively involved in internalizing foreign particles, which makes them prone to oxidative fluctuations and membrane destabilization, key mechanisms of particle-induced cytotoxicity. In contrast, hyalinocytes exhibit lower phagocytic capacity, reducing their susceptibility to these cytotoxic mechanisms (Canesi et al., 2012; He et al., 2023; Le Foll et al., 2010). The absence of significant hemocyte mortality at later exposure time points and during the recovery period suggests the activation of cellular repair mechanisms. Recent studies suggested that bivalves can exhibit a shift in immune parameters and reestablish basal functions to restore immune homeostasis after repeated exposure to 50 nm PS-NH_2 (10 μg/L or 1.46×10^{11} particles/L) (Auguste et al., 2020). It is worth noting, however, that MNP-induced cytotoxicity in hemocytes may be exacerbated or mitigated when co-exposed with other associated contaminants, highlighting the complexity of these interactions in real-world conditions (Mkuye et al., 2022). Additionally, simultaneous exposure to global change-driven stressors, such as ocean warming, acidification, deoxygenation, and marine heat waves, can intensify stress responses (Catarino et al., 2022). Impairment in cellular immunity under these compounded stressors has significant consequences, such as increased susceptibility to pathogen infections. These cascading effects can extend beyond individual organisms, influencing populations, communities, and entire ecosystems (Kataoka and Kashiwada, 2021).

4.2. Tissue alterations induced by aged PET MNP exposure

Several studies have reported that MNPs, including high-density polyethylene (HDPE, ≤ 22 μm, mean 4–6 μm), PS (3 μm, 9.6 μm), PE (10.7–93.9 μm), and pristine PET (9.0–56.0 μm), exhibit efficient particle clearance and tissue accumulation dynamics in bivalves (see Supplementary Table A.3 for exposure details) (Browne et al., 2008; Fernández and Albentosa, 2019a; Teng et al., 2021b). Notably, mussels have been reported to exhibit size-dependent accumulation, with 0.07 μm PS particles demonstrating significantly higher retention in the digestive tract compared to larger particles (Wang et al., 2021). Despite partial elimination during depuration, smaller MNPs persist in critical organs, such as the digestive gland and gills of mussels (Browne et al., 2008; Fernández and Albentosa, 2019a, 2019b). Histopathological changes in these organs are widely recognized as sensitive biomarkers of environmental stress and pollution, offering insights into organismal health (Ertürk Gürkan and Gürkan, 2021). The current study builds on this knowledge, revealing the differential histopathological responses of these organs to aged PET MNP (C3) exposure.

While no significant increase was observed in the histopathological condition index, notable alterations were evident in the digestive glands of exposed mussels. Most prominently, an increased prevalence of atrophied tubules was observed, with thinner epithelium and an enlarged lumen (Cuevas et al., 2015). Mussels (*M. galloprovincialis)* exposed to virgin and weathered PE fragments (50–590 μm; 1180 and 1186 particles/L, 21 days) and PET microfibers (20–140 μm; 6.1×10^5 particles/L and 6.1×10^6 particles/L, 32 days) also exhibited digestive tubule atrophy (Bråte et al., 2018; Choi et al., 2022). Similarly, exposure to 200 nm PS NPs particularly at concentrations of 200 μg/L (4.55×10^{10} particles/L) and 2000 μg/L (4.55×10^{11} particles/L) for 14 days induced thinner epithelia, barren digestive cells, wider lumens, and exfoliated cells. These changes in the digestive tubule morphology and planimetric parameters have been linked to severely disrupted metabolic capability (Lu et al., 2023b). Such regressive changes occur in association with cellular degeneration and necrotic processes and can lead to impaired digestive function (Carella et al., 2015).

In the present work, exposure to the highest concentration of aged PET MNPs induced pronounced histopathological alterations in the gills, accompanied by significant increases in I_h values during both exposure and recovery periods. Key alterations, such as lamellar fusion and the enlargement of the central vessels, were prominently observed. Lamellar fusions were observed across the lateral and abfrontal zones of the gill filaments, which are critical for water pumping, lubrication, gill cleaning, gas exchange, and particle trapping (Leis et al., 2024). Similar severe alterations, including damaged inter-lamellar junctions, epithelial loss, and swollen lumens, were reported in gills of mussels (*Perna viridis*) exposed to weathered PE particles (15 % <32 μm and 85 % 32–43 μm, at 1150–3360 particles/m^3 or 1.15–3.36 particles/L) for 30 days. These structural alterations highlight the potential impairment of essential gill functions, including respiration, osmoregulation, and filtration efficiency (Hariharan et al., 2021). Inflammatory responses, evidenced by hemocyte infiltration in epithelial layer or hemolymph vessels, exacerbated the structural damage and correlated with diffuse gill inflammation. Exposure to 10–1000 μg/L of irregularly-shaped PE (10.7–93.9 μm, 4.19×10^2–4.19×10^4 particles/L) and PET (9.0–56.0 μm, 4.60×10^2–4.60×10^4 particles/L) induced severe hemocyte infiltration in the gills of oysters (*Crassostrea gigas*) (Teng et al., 2021b). Extensive hemocyte infiltration alters lamellar structure through overcrowding and cause recurrent enlargement of the hemolymphatic vessels (Costa et al., 2013; Leis et al., 2024). Interestingly, gill filament deformation may also occur without hemocytic intrusion, likely representing an early-stage inflammatory response that precedes hemocyte invasion of the target site (Bouallegui et al., 2017).

Lipofuscin aggregates, particularly observed in digestive tubules and gill filaments exhibiting regressive changes, suggest a heightened oxidative imbalance (Leis et al., 2024). Formed through iron-catalyzed oxidative processes, lipofuscin is a non-degradable intralysosomal, polymeric substance composed of cross-linked protein and lipid residues. Its indigestible nature is associated with progressive lysosomal dysfunction, with cascading effects on various cellular activities. Its accumulation can interfere with autophagy by serving as a sink for newly produced lysosomal enzymes, which in turn hinders the recycling of cellular components. This disruption prevents effective cellular renewal, exacerbates the accumulation of damaged cellular constituents, and ultimately advances tissue degeneration (Brunk and Terman, 2002). The presence of these aggregates potentially indicates localized oxidative stress in tissues directly interacting with MNPs (Leis et al., 2024).

Varying degrees of histopathological alterations induced by MNPs have been documented in mussel tissues. For instance, *Mytilus coruscus* exposed to 20 mg/L PS MPs (1 μm, 3.64×10^{10} particles/L) exhibited less severe digestive tissue damage than PS NPs (100 nm, 3.64×10^{13} particles/L) (Qi et al., 2023). Similarly, 7-day exposure to PS (2–6 μm, 32 μg/L; 2.0×10^6 particles/L) alone or combined with fluoranthene (30 μg/L, 1.5×10^{-7} M) significantly increased histopathological lesions, with persistent hemocyte infiltration and lipofuscin aggregation after the depuration period, especially in co-exposure group (Paul-Pont et al., 2016). Weathered PE particles (15 % <32 μm and 85 % 32–43 μm, at 1150–3360 particles/m^3 or 1.15–3.36 particles/L) also caused comparable lesions, with minimal recovery even after a 7-day depuration period (Hariharan et al., 2021). The persistence of these moderate lesions post-exposure underscores delayed or incomplete tissue repair within the tested experimental duration, potentially indicating a prolonged physiological burden from particle exposure. Consequently, the alterations observed in this study could be attributed to the physical properties of aged PET particles, particularly surface irregularities, which may induce mechanical abrasion. A recent study reported that PET induced a higher damage index than PE in both tissues, attributed to its more angular and rough edges (Teng et al., 2021b).

To contextualize the histopathological effects of aged PET MNPs, comparisons with tissue-specific damage indices for other particulate toxicants in mussels are essential. For instance, exposure to gamma aluminum oxide (γ-Al_2O, 5 nm, 5–40 mg/L or 1.93×10^{16}–1.54×10^{17} particles/L) for 4 days caused severe damage in both organs, with mean I_h values within the high to very high category (Ertürk Gürkan and Gürkan, 2021). Exposure to lanthanum (La) in the form of dissolved ions for 28 days exhibit progressive, dose-dependent damage, with gill I_h values rising from moderate (0.1 mg/L or 7.2×10^{-7} M) to high (1.0–10.0 mg/L or 7.2×10^{-6} M–7.2×10^{-5} M) and digestive gland values progressing from low to moderate at the same concentrations (Pinto et al., 2019). Interestingly, exposure to 10 μg/L cadmium-based quantum dots (CdTe QDs, 6 nm, 1.43×10^{13} particles/L) and dissolved Cd (8.9×10^{-8} M) counterparts for 14 days significantly increased digestive gland I_h compared to controls, while remaining within the low category except for dissolved Cd (Rocha et al., 2016). These analyses provide insights into the severity and nature of tissue damage, influenced by particle properties, exposure conditions, and uptake routes, with critical implications for organismal health (Bouallegui et al., 2018).

4.3. Implications for organismal health

While cellular and tissue level analyses exhibited differential sensitivities, no significant effects on survival or growth metrics were observed following exposure to aged PET MNPs. Similarly, a 21-day exposure of mussels (*M. galloprovincialis*) to virgin and weathered PE (50–590 μm at 1180 and 1186 particles/L, respectively) caused no mortality or changes in condition index, despite evidence of histopathological alterations (Bråte et al., 2018). Exposure to 10 and 1000 μg/L of irregularly-shaped PE (10.7–93.9 μm, 4.19×10^2–4.19×10^4 particles/L) and PET (9.0–56.0 μm, 4.60×10^2–4.60×10^4 particles/L) for 21 days similarly showed no significant effects on the condition index in oysters (*C. gigas*) (Teng et al., 2021a), though changes in histopathological parameters, lipid metabolism biomarkers, and cell membrane integrity, were observed (Teng et al., 2021b). In contrast, exposure to 40–48 μm virgin PE at 100 μg/L (1.88–3.24×10^3 particles/L) and 1000 μg/L (1.88–3.24×10^4 particles/L) for 14 days caused significant weight loss and immune alterations without inducing mortality in other bivalve species (*Ruditapes decussatus*) (Abidli et al., 2023).

The variability in responses highlights the critical role of particle characteristics, such as size, shape, and weathering state, along with exposure duration and concentration, in determining the mode and extent of MNP-induced effects. Aging processes significantly alter the surface and physicochemical properties of plastic particles, influencing environmental behavior and interaction with organisms. These alterations, including fragmentation into smaller particles, discoloration, formation of oxygen-containing groups, and biofilm development, can modulate their biological impacts (Liu et al., 2020). For instance, plastic particles smaller than 4 μm have been reported to accumulate in the digestive gland of mussels, exhibiting longer retention times and higher translocation rates to the circulatory system compared to larger particles (Browne et al., 2008; Fernández and Albentosa, 2019a, 2019b). In mussels, two distinct pathways for plastic particle uptake have been reported. The first involves direct transport through gill surfaces, via microvilli-mediated endocytosis, primarily for smaller particles. The second pathway relies on ciliary movement to transfer particles through the digestive system, including the stomach, intestine, and ultimately the digestive gland ducts and tubules (Von Moos et al., 2012).

The histopathological alterations observed in gills and digestive gland align with previous findings, underscoring the susceptibility of these tissues to MNP exposure (Barría et al., 2025). While the observed recovery at the cellular level suggests that bivalves exhibit compensatory mechanisms to alleviate stress after an acute exposure event (Auguste et al., 2020). Moreover, differences in gene expression observed between single and repetitive exposures to HDPE (1–50 μm, 4.6×10^5 particles/L) highlight the development of stress memory. However, the increased energy demands associated with repeated high-concentration exposure raise concerns about the sustainability of

these mechanisms. Chronic exposure to elevated MNP levels could overwhelm the organisms' physiological resilience, leading to impaired fitness, and potentially compromising long-term population viability (Détrée and Gallardo-Escárate, 2018).

Additionally, the interplay between MNPs and other environmental stressors, such as chemical pollutants, may exacerbate or mitigate their physiological impacts (Mkuye et al., 2022). MNPs' capability to impair essential biological functions, when combined with other stressors, could potentially propagate adverse effects beyond the organismal level. One potential major problem is the ability of MNPs to accumulate toxic compounds, either adsorbed from the environment or retained during manufacturing processes (Barría et al., 2025). Contaminated PE and PS have been reported to transfer PAHs to exposed mussels, increasing bioavailability post-ingestion and inducing toxicological effects at molecular and cellular levels (Avio et al., 2015). In some cases, MNPs may reduce the bioavailability of other organic compounds, depending on inherent particle properties, and interactions within the exposure medium and the organism. This highlights the need for further research on MNP-contaminant interactions across diverse scenarios (Tang, 2021).

4.4. Conclusions, limitations, and future directions

This study provides an integrative analysis of the cellular and tissue-level responses of the blue mussel (*M. edulis*) to aged PET MNP under environmentally relevant conditions, offering valuable insights into the underlying mechanisms of toxicity associated with aged particles. Current findings revealed the sensitivity of hemocyte subpopulations, including granulocytes and hyalinocytes, following exposure to aged PET MNPs. Concentration- and time-dependent changes in lysosomal stability, oxidative activity, and hemocyte mortality were observed, demonstrating both immediate cellular perturbations and recovery potential to alleviate particle-induced effects. Histopathological analysis indicated significant alterations, particularly in the gill tissues, suggesting potential impairment of essential physiological functions. No mortality or significant changes in growth metrics were observed in mussels following exposure to aged PET MNPs. Notably, the magnitude of these observed responses aligns with those reported for different types of MNPs and other materials, under similar exposure concentrations and durations.

While this study provides valuable insights into the physiological responses associated with aged MNP exposure, certain limitations must be acknowledged. The detection and quantification of aged MNPs in complex matrices remain a challenge due to analytical constraints (Cunningham et al., 2023; da Costa et al., 2019). Although techniques such as Nile red staining coupled with machine learning have shown potential for detecting MNPs in mussel tissues, the recently developed polymer identification model (PIM) exhibited lower predictive accuracy for PET particles compared to other polymers. PIM is a semi-automated technique designed to classify four polymer categories (PE/PP, PS, PET, and PVC) through fluorescent particle staining following tissue digestion and filtration (Meyers et al., 2024). Histopathological indices, while informative and effective, may not detect rare and early-stage precursor lesions linked to particle exposure. Long-term mechanistic studies are needed to assess a broader range of sub-lethal effects associated with aged MNPs, including immunotoxicity, reproductive and transgenerational toxicity, as well as to elucidate potential recovery processes following chronic exposure (He et al., 2023; Yi et al., 2024). Importantly, future research should incorporate environmentally relevant exposure scenarios, particularly co-exposure with other contaminants (e.g., persistent organic pollutants) (Wang et al., 2020) and global change-related stressors (e.g., ocean warming and acidification) (Catarino et al., 2022), to better capture potential synergistic or antagonistic interactions that may modulate toxicity outcomes. These efforts are essential for understanding the combined effects of these stressors and conducting robust risk assessments for aged MNP exposure (Cunningham et al., 2023).

CRediT authorship contribution statement

Jenevieve Hara: Writing – review & editing, Writing – original draft, Visualization, Methodology, Investigation, Formal analysis, Data curation, Conceptualization. **Gethrie B. Oraño:** Writing – original draft, Visualization, Methodology, Investigation, Formal analysis, Data curation. **Maaike Vercauteren:** Writing – review & editing, Methodology, Formal analysis, Conceptualization. **Kayawe Valentine Mubiana:** Writing – review & editing, Methodology, Investigation, Formal analysis. **Colin R. Janssen:** Supervision, Funding acquisition. **Ronny Blust:** Supervision, Methodology, Funding acquisition. **Jana Asselman:** Writing – review & editing, Supervision, Funding acquisition, Conceptualization. **Raewyn M. Town:** Writing – review & editing, Supervision, Methodology, Funding acquisition, Conceptualization.

Declaration of competing interest

The authors declare that they have no known competing financial interests or personal relationships that could have appeared to influence the work reported in this paper.

Acknowledgments

Jenevieve Hara is supported by the RESPONSE project, funded under the Joint Action Ecological Aspects of Microplastics of JPI Oceans (B2/20E/P1/ RESPONSE "Toward a risk-based assessment of microplastic pollution in marine ecosystems") and Research Foundation - Flanders (FWO) (G053320N "Towards ecological risk assessment of nanoplastics: dynamic considerations). Gethrie Oraño is funded by the Erasmus+ scholarship program (MAEH). Maaike Vercauteren is funded by the Special Research Fund of Ghent University (Grant BOF21/PDO/081). Test particles and the primary characterization were supplied by the Joint Research Centre (JRC), with the support of John Seghers, Håkan Emteborg, and Claudia Cella. We thank the experts at the Antwerp Centre for Advanced Microscopy (Sofie Thys, Isabel Pintelon, and Prof. Jean-Pierre Timmermans) for their invaluable support with tissue processing and histopathological analysis.

Supplementary materials

Supplementary material associated with this article can be found, in the online version, at doi:10.1016/j.aquatox.2025.107369.

Data availability

Data will be made available on request.

References

Abidli, S., Zaidi, S., Ben Younes, R., Lahbib, Y., Trigui El Menif, N., 2023. Impact of polyethylene microplastics on the clam *Ruditapes decussatus* (Mollusca: bivalvia): examination of filtration rate, growth, and immunomodulation. Ecotoxicology 32 (6), 746–755. https://doi.org/10.1007/s10646-023-02683-2.

Ashrafy, A., Liza, A.A., Islam, M.N., Billah, M.M., Arafat, S.T., Rahman, M.M., Rahman, S. M., 2023. Microplastics pollution: a brief review of its source and abundance in different aquatic ecosystems. J. Hazard. Mater. Adv. 9. https://doi.org/10.1016/j.hazadv.2022.100215.

Auguste, M., Balbi, T., Ciacci, C., Canonico, B., Papa, S., Borello, A., Vezzulli, L., Canesi, L., 2020. Shift in immune parameters after repeated exposure to nanoplastics in the marine Bivalve Mytilus. Front. Immunol. 11. https://doi.org/10.3389/fimmu.2020.00426.

Avio, C.G., Gorbi, S., Milan, M., Benedetti, M., Fattorini, D., D'Errico, G., Pauletto, M., Bargelloni, L., Regoli, F., 2015. Pollutants bioavailability and toxicological risk from microplastics to marine mussels. Environ. Pollut. 198, 211–222. https://doi.org/10.1016/j.envpol.2014.12.021.

Barría, C., Balasch, J.C., Brandts, I., Oliva, D., Iriarte, J.L., Teles, M., 2025. Immunological responses, oxidative stress, and histopathological effects of nanoplastics on commercially relevant mussel species: a review. J. Hazard. Mater. Adv. 17. https://doi.org/10.1016/j.hazadv.2024.100540.

Besseling, E., Redondo-Hasselerharm, P., Foekema, E.M., Koelmans, A.A., 2019. Quantifying ecological risks of aquatic micro- and nanoplastic. Crit. Rev. Environ. Sci. Technol. 49 (1), 32–80. https://doi.org/10.1080/10643389.2018.1531688.

Beyer, J., Green, N.W., Brooks, S., Allan, I.J., Ruus, A., Gomes, T., Bråte, I.L.N., Schøyen, M., 2017. Blue mussels (Mytilus edulis spp.) as sentinel organisms in coastal pollution monitoring: a review. Mar. Environ. Res. 130, 338–365. https://doi.org/10.1016/j.marenvres.2017.07.024.

Bouallegui, Y., Ben Younes, R., Bellamine, H., Oueslati, R., 2017. Histopathology and analyses of inflammation intensity in the gills of mussels exposed to silver nanoparticles: role of nanoparticle size, exposure time, and uptake pathways. Toxicol. Mech. Methods 27 (8), 582–591. https://doi.org/10.1080/15376516.2017.1337258.

Bouallegui, Y., Ben Younes, R., Bellamine, H., Oueslati, R., 2018. Histopathological indices and inflammatory response in the digestive gland of the mussel mytilus galloprovincialis as biomarker of immunotoxicity to silver nanoparticles. Biomarkers 23 (3), 277–287. https://doi.org/10.1080/1354750X.2017.1409803.

Bråte, I.L.N., Blázquez, M., Brooks, S.J., Thomas, K.V., 2018. Weathering impacts the uptake of polyethylene microparticles from toothpaste in Mediterranean mussels (M. galloprovincialis). Sci. Total Environ. 626, 1310–1318. https://doi.org/10.1016/j.scitotenv.2018.01.141.

Browne, M.A., Dissanayake, A., Galloway, T.S., Lowe, D.M., Thompson, R.C., 2008. Ingested microscopic plastic translocates to the circulatory system of the mussel, Mytilus edulis (L.). Environ. Sci. Technol. 42 (13), 5026–5031. https://doi.org/10.1021/es800249a.

Brunk, U.T., Terman, A., 2002. Lipofuscin: mechanism of aged-related accummulation and influence on cell function. Free Radic. Biol. Med. https://doi.org/10.1016/S0891-5849(02)00959-0.

Canesi, L., Ciacci, C., Bergami, E., Monopoli, M.P., Dawson, K.A., Papa, S., Canonico, B., Corsi, I., 2015. Evidence for immunomodulation and apoptotic processes induced by cationic polystyrene nanoparticles in the hemocytes of the marine bivalve Mytilus. Mar. Environ. Res. 111, 34–40. https://doi.org/10.1016/j.marenvres.2015.06.008.

Canesi, L., Ciacci, C., Fabbri, R., Marcomini, A., Pojana, G., Gallo, G., 2012. Bivalve molluscs as a unique target group for nanoparticle toxicity. Mar. Environ. Res. 76, 16–21. https://doi.org/10.1016/j.marenvres.2011.06.005.

Canesi, L., Procházková, P., 2014. The invertebrate immune system as a model for investigating the environmental impact of nanoparticles. Nanoparticles and the Immune System. Academic Press, pp. 91–112. https://doi.org/10.1016/B978-0-12-408085-0.00007-8.

Capolupo, M., Valbonesi, P., Fabbri, E., 2021. A comparative assessment of the chronic effects of micro-and nano-plastics on the physiology of the mediterranean mussel mytilus galloprovincialis. Nanomaterials 11 (3), 1–17. https://doi.org/10.3390/nano11030649.

Carella, F., Feist, S.W., Bignell, J.P., De Vico, G., 2015. Comparative pathology in bivalves: aetiological agents and disease processes. J. Invertebr. Pathol. 131, 107–120. https://doi.org/10.1016/j.jip.2015.07.012.

Catarino, A.I., Asselman, J., Niu, Z., Everaert, G., 2022. Micro- and nanoplastics effects in a multiple stressed marine environment. J. Hazard. Mater. Adv. 7. https://doi.org/10.1016/j.hazadv.2022.100119.

Chen, J.-H., Bayne, C.J., 1995. Bivalve mollusc hemocyte behaviors: characterization of hemocyte aggregation and adhesion and their inhibition in the California mussel (Mytilus californianus). Biol. Bull 188, 255–266. https://doi.org/10.2307/1542303.

Choi, J.S., Kim, K., Park, K., Park, J.W., 2022. Long-term exposure of the Mediterranean mussels, Mytilus galloprovincialis to polyethylene terephthalate microfibers: implication for reproductive and neurotoxic effects. Chemosphere 299. https://doi.org/10.1016/j.chemosphere.2022.134317.

Costa, P.M., Carreira, S., Costa, M.H., Caeiro, S., 2013. Development of histopathological indices in a commercial marine bivalve (Ruditapes decussatus) to determine environmental quality. Aquat. Toxicol. 126, 442–454. https://doi.org/10.1016/j.aquatox.2012.08.013.

Cuevas, N., Zorita, I., Costa, P.M., Franco, J., Larreta, J., 2015. Development of histopathological indices in the digestive gland and gonad of mussels: integration with contamination levels and effects of confounding factors. Aquat. Toxicol. 162, 152–164. https://doi.org/10.1016/j.aquatox.2015.03.011.

Cunningham, B.E., Sharpe, E.E., Brander, S.M., Landis, W.G., Harper, S.L., 2023. Critical gaps in nanoplastics research and their connection to risk assessment. Front. Toxicol. 5. https://doi.org/10.3389/ftox.2023.1154538.

da Costa, J.P., Reis, V., Paço, A., Costa, M., Duarte, A.C., Rocha-Santos, T., 2019. Micro (nano)plastics – analytical challenges towards risk evaluation. TrAC - Trends Anal. Chem. 111, 173–184. https://doi.org/10.1016/j.trac.2018.12.013.

de la Ballina, N.R., Maresca, F., Cao, A., Villalba, A., 2022. Bivalve haemocyte subpopulations: a review. Front. Immunol. 13. https://doi.org/10.3389/fimmu.2022.826255.

De Ruijter, V.N., Redondo-Hasselerharm, P.E., Gouin, T., Koelmans, A.A., 2020. Quality criteria for microplastic effect studies in the context of risk assessment: a critical review. Environ. Sci. Technol. 54 (19), 11692–11705. https://doi.org/10.1021/acs.est.0c03057.

Détrée, C., Gallardo-Escárate, C., 2018. Single and repetitive microplastics exposures induce immune system modulation and homeostasis alteration in the edible mussel Mytilus galloprovincialis. Fish Shellfish Immunol. 83, 52–60. https://doi.org/10.1016/j.fsi.2018.09.018.

Ertürk Gürkan, S., Gürkan, M., 2021. Toxicity of gamma aluminium oxide nanoparticles in the Mediterranean mussel (Mytilus galloprovincialis): histopathological alterations and antioxidant responses in the gill and digestive gland. Biomarkers 26 (3), 248–259. https://doi.org/10.1080/1354750X.2021.1878558.

Fernández, B., Albentosa, M., 2019a. Dynamic of small polyethylene microplastics (≤10 μm) in mussel's tissues. Mar. Pollut. Bull. 146, 493–501. https://doi.org/10.1016/j.marpolbul.2019.06.021.

Fernández, B., Albentosa, M., 2019b. Insights into the uptake, elimination and accumulation of microplastics in mussel. Environ. Pollut. 249, 321–329. https://doi.org/10.1016/j.envpol.2019.03.037.

Fraissinet, S., De Benedetto, G.E., Malitesta, C., Holzinger, R., Materić, D., 2024. Microplastics and nanoplastics size distribution in farmed mussel tissues. Commun. Earth Environ. 5 (1). https://doi.org/10.1038/s43247-024-01300-2.

Galloway, T.S., Cole, M., Lewis, C., 2017. Interactions of microplastic debris throughout the marine ecosystem. Nat. Ecol. Evol. 1 (5), 1–8. https://doi.org/10.1038/s41559-017-0116.

Hara, J., Vercauteren, M., Schoenaers, S., Janssen, C.R., Blust, R., Asselman, J., Town, R. M., 2024. Differential sensitivity of hemocyte subpopulations (Mytilus edulis) to aged polyethylene terephthalate micro- and nanoplastic particles. Ecotoxicol. Environ. Saf. 286. https://doi.org/10.1016/j.ecoenv.2024.117255.

Hariharan, G., Purvaja, R., Anandavelu, I., Robin, R.S., Ramesh, R., 2021. Accumulation and ecotoxicological risk of weathered polyethylene (wPE) microplastics on green mussel (Perna viridis). Ecotoxicol. Environ. Saf. 208. https://doi.org/10.1016/j.ecoenv.2020.111765.

He, T., Qu, Y., Yang, X., Liu, L., Xiong, F., Wang, D., Liu, M., Sun, R., 2023. Research progress on the cellular toxicity caused by microplastics and nanoplastics. J. Appl. Toxicol. 43 (11), 1576–1593. https://doi.org/10.1002/jat.4449.

Hu, M., Palić, D., 2020. Micro- and nano-plastics activation of oxidative and inflammatory adverse outcome pathways. Redox. Biol. 37, 101620. https://doi.org/10.1016/j.redox.2020.101620.

Huang, X., Leung, J.Y.S., Hu, M., Xu, E.G., Wang, Y., 2022. Microplastics can aggravate the impact of ocean acidification on the health of mussels: insights from physiological performance, immunity and byssus properties. Environ. Pollut. 308. https://doi.org/10.1016/j.envpol.2022.119701.

Jeon, S., Lee, D.K., Jeong, J., Yang, S.I., Kim, J.S., Kim, J., Cho, W.S., 2021. The reactive oxygen species as pathogenic factors of fragmented microplastics to macrophages. Environ. Pollut. 281, 117006. https://doi.org/10.1016/j.envpol.2021.117006.

Kataoka, C., Kashiwada, S., 2021. Ecological risks due to immunotoxicological effects on aquatic organisms. Int. J. Mol. Sci. 22 (15). https://doi.org/10.3390/ijms22158305.

Khanna, R., Chandra, A., Sen, S., Konyukhov, Y., Fuentes, E., Burmistrov, I., Kravchenko, M., 2024. Microplastics and nanoplastics as environmental contaminants of emerging concern: potential hazards for human health. Sustainability 16 (19). https://doi.org/10.3390/su16198704.

Le Foll, F., Rioult, D., Boussa, S., Pasquier, J., Dagher, Z., Leboulenger, F., 2010. Characterisation of mytilus edulis hemocyte subpopulations by single cell time-lapse motility imaging. Fish Shellfish Immunol. 28 (2), 372–386. https://doi.org/10.1016/j.fsi.2009.11.011.

Leis, M., Noya Abad, T., Martinez, M.F., Calcagno, J.A., Sabatini, S.E., Genovese, G., 2024. Histological alterations as a recommended biomarker in the mussel Mytilus platensis (Bivalvia, Mytilidae) to study anthropic impact on seaports. Reg. Stud. Mar. Sci. 70. https://doi.org/10.1016/j.rsma.2024.103373.

Lenz, R., Enders, K., Nielsen, T.G., 2016. Microplastic exposure studies should be environmentally realistic. Proc. Natl. Acad. Sci. U.S.A. 113 (29), E4121–E4122. https://doi.org/10.1073/pnas.1606615113.

Li, L.L., Amara, R., Souissi, S., Dehaut, A., Duflos, G., Monchy, S., 2020. Impacts of microplastics exposure on mussel (Mytilus edulis) gut microbiota. Sci. Total Environ. 745. https://doi.org/10.1016/j.scitotenv.2020.141018.

Li, X., Wu, H., Gong, J., Li, Q., Li, Z., Zhang, J., 2023. Improvement of biodegradation of PET microplastics with whole-cell biocatalyst by interface activation reinforcement. Environ. Technol. 44 (20), 3121–3130. https://doi.org/10.1080/09593330.2022.2052359 *(United Kingdom)*.

Li, Z., Chang, X., Hu, M., Fang, J.K.H., Sokolova, I.M., Huang, W., Xu, E.G., Wang, Y., 2022. Is microplastic an oxidative stressor? Evidence from a meta-analysis on bivalves. J. Hazard. Mater. 423. https://doi.org/10.1016/j.jhazmat.2021.127211.

Liu, P., Zhan, X., Wu, X., Li, J., Wang, H., Gao, S., 2020. Effect of weathering on environmental behavior of microplastics: properties, sorption and potential risks. Chemosphere 242. https://doi.org/10.1016/j.chemosphere.2019.125193.

Lu, Q., Zhou, Y., Sui, Q., Zhou, Y., 2023a. Mechanism and characterization of microplastic aging process: a review. Front. Environ. Sci. Eng. 17 (8). https://doi.org/10.1007/s11783-023-1700-6.

Lu, Z., Wu, S., Xiao, Z., Song, J., Wu, H., Peng, X., 2023b. Responses of microRNA in digestive glands of mussel mytilus galloprovincialis exposed to polystyrene nanoplastics. Ecotoxicol. Environ. Saf. 249. https://doi.org/10.1016/j.ecoenv.2022.114412.

Luo, Y., Wang, W.X., 2022. Immune responses of oyster hemocyte subpopulations to in vitro and in vivo zinc exposure. Aquat. Toxicol. 242, 106022. https://doi.org/10.1016/j.aquatox.2021.106022.

Meyers, N., Everaert, G., Hostens, K., Schmidt, N., Herzke, D., Fuda, J.L., Janssen, C.R., De Witte, B., 2024. Towards reliable data: validation of a machine learning-based approach for microplastics analysis in marine organisms using Nile red staining. Mar. Pollut. Bull. 207. https://doi.org/10.1016/j.marpolbul.2024.116804.

Mkuye, R., Gong, S., Zhao, L., Masanja, F., Ndandala, C., Bubelwa, E., Yang, C., Deng, Y., 2022. Effects of microplastics on physiological performance of marine bivalves, potential impacts, and enlightening the future based on a comparative study. Sci. Total Environ. 838. https://doi.org/10.1016/j.scitotenv.2022.155933.

Moore, M.N., Allen, J.I., McVeigh, A., Shaw, J., 2006. Lysosomal and autophagic reactions as predictive indicators of environmental impact in aquatic animals. Autophagy 2 (3), 217–220. https://doi.org/10.4161/auto.2663.

Olabarrieta, I., L'azou, B., Yuric, S., Cambar, J., Cajaraville, M.P., Zelularra, B., Laborategia, H., Eta, Z., Zelulen, A., Saila, D., Fakultatea, Z., 2001. In vitro effects of

cadmium on two different animal cell models. *Toxicol.* In Vitro 15, 511–517. https://doi.org/10.1016/S0887-2333(01)00056-X.

Paul-Pont, I., Lacroix, C., González Fernández, C., Hégaret, H., Lambert, C., Le Goïc, N., Frère, L., Cassone, A.L., Sussarellu, R., Fabioux, C., Guyomarch, J., Albentosa, M., Huvet, A., Soudant, P., 2016. Exposure of marine mussels mytilus spp. to polystyrene microplastics: toxicity and influence on fluoranthene bioaccumulation. Environ. Pollut. 216, 724–737. https://doi.org/10.1016/j.envpol.2016.06.039.

Pinto, J., Costa, M., Leite, C., Borges, C., Coppola, F., Henriques, B., Monteiro, R., Russo, T., Di Cosmo, A., Soares, A.M.V.M., Polese, G., Pereira, E., Freitas, R., 2019. Ecotoxicological effects of lanthanum in Mytilus galloprovincialis: biochemical and histopathological impacts. Aquat. Toxicol. 211, 181–192. https://doi.org/10.1016/j.aquatox.2019.03.017.

Qi, P., Qiu, L., Feng, D., Gu, Z., Guo, B., Yan, X., 2023. Distinguish the toxic differentiations between acute exposure of micro- and nano-plastics on bivalves: an integrated study based on transcriptomic sequencing. Aquat. Toxicol. 254. https://doi.org/10.1016/j.aquatox.2022.106367.

Revel, M., Roman, C., Châtel, A., 2021. Is cell culture a suitable tool for the evaluation of micro- and nanoplastics ecotoxicity? Ecotoxicology 30 (3), 421–430. https://doi.org/10.1007/s10646-021-02355-z.

Ribeiro, F., O'Brien, J.W., Galloway, T., Thomas, K.V., 2019. Accumulation and fate of nano- and micro-plastics and associated contaminants in organisms. TrAC - Trends Anal. Chem. 111, 139–147. https://doi.org/10.1016/j.trac.2018.12.010.

Riisgard, H.U., 1991. Filtration rate and growth in the blue mussel, Mytilus edulis Linnaeaus, 1758: dependence on algal concentration. J. Shellfish Res. 10 (1), 29–35.

Riisgard, H.U., Egede, P.P., Saavedra, I.B., 2011. Feeding behaviour of the Mussel, Mytilus edulis: new observations, with a minireview of current knowledge. J. Mar. Sci. 2011. https://doi.org/10.1155/2011/312459.

Rocha, T.L., Sabóia-Morais, S.M.T., Bebianno, M.J., 2016. Histopathological assessment and inflammatory response in the digestive gland of marine mussel mytilus galloprovincialis exposed to cadmium-based quantum dots. Aquat. Toxicol. 177, 306–315. https://doi.org/10.1016/j.aquatox.2016.06.003.

Roman, C., Mahé, P., Latchere, O., Catrouillet, C., Gigault, J., Métais, I., Châtel, A., 2023. Effect of size continuum from nanoplastics to microplastics on marine mussel mytilus edulis: comparison in vitro/in vivo exposure scenarios. Comp. Biochem. Physiol. Part - C Toxicol. Pharmacol. 264, 109512. https://doi.org/10.1016/j.cbpc.2022.109512.

Santana, M.F.M., Moreira, F.T., Pereira, C.D.S., Abessa, D.M.S., Turra, A., 2018. Continuous exposure to microplastics does not cause physiological effects in the cultivated mussel *Perna perna*. Arch. Environ. Contam. Toxicol. 74 (4), 594–604. https://doi.org/10.1007/s00244-018-0504-3.

Seghers, J., Cella, C., Pequeur, E., La Spina, R., Roncari, F., Valsesia, A., Mehn, D., Gilliland, D., Trapmann, S., Emteborg, H., 2025. Approaches for the preparation and evaluation of hydrophilic polyethylene and polyethylene terephthalate microplastic particles suited for toxicological effect studies. Anal. Bioanal. Chem. https://doi.org/10.1007/s00216-024-05726-7.

Sendra, M., Carrasco-Braganza, M.I., Yeste, P.M., Vila, M., Blasco, J., 2020. Immunotoxicity of polystyrene nanoplastics in different hemocyte subpopulations of Mytilus galloprovincialis. Sci. Rep. 10 (1), 1–14. https://doi.org/10.1038/s41598-020-65596-8.

Sioen, M., Vercauteren, M., Blust, R., Town, R.M., Janssen, C., Asselman, J., 2024. Impact of weathered and virgin polyethylene terephthalate (PET) micro- and nanoplastics on growth dynamics and the production of extracellular polymeric substances (EPS) of microalgae. Sci. Total Environ. 953. https://doi.org/10.1016/j.scitotenv.2024.176074.

Tang, K.H.D., 2021. Interactions of microplastics with persistent organic pollutants and the ecotoxicological effects: a review. Trop. Aquat. Soil Pollut. 1 (1), 24–34. https://doi.org/10.53623/tasp.v1i1.11.

Teng, J., Zhao, J., Zhu, X., Shan, E., Wang, Q., 2021a. Oxidative stress biomarkers, physiological responses and proteomic profiling in oyster (Crassostrea gigas) exposed to microplastics with irregular-shaped PE and PET microplastic. Sci. Total Environ. 786. https://doi.org/10.1016/j.scitotenv.2021.147425.

Teng, J., Zhu, X., Shan, E., Zhang, C., Zhang, W., Wang, Q., 2021b. Toxic effects of exposure to microplastics with environmentally relevant shapes and concentrations: accumulation, energy metabolism and tissue damage in oyster crassostrea gigas. Environ. Pollut. 269, 116169. https://doi.org/10.1016/j.envpol.2020.116169.

Von Moos, N., Burkhardt-Holm, P., Köhler, A., 2012. Uptake and effects of microplastics on cells and tissue of the blue mussel Mytilus edulis L. after an experimental exposure. Environ. Sci. Technol. 46 (20), 11327–11335. https://doi.org/10.1021/es302332w.

Wang, S., Hu, M., Zheng, J., Huang, W., Shang, Y., Kar-Hei Fang, J., Shi, H., Wang, Y., 2021. Ingestion of nano/micro plastic particles by the mussel Mytilus coruscus is size dependent. Chemosphere 263. https://doi.org/10.1016/j.chemosphere.2020.127957.

Wang, T., Huang, X., Jiang, X., Hu, M., Huang, W., Wang, Y., 2019. Differential in vivo hemocyte responses to nano titanium dioxide in mussels: effects of particle size. Aquat. Toxicol. 212, 28–36. https://doi.org/10.1016/j.aquatox.2019.04.012.

Wang, T., Wang, L., Chen, Q., Kalogerakis, N., Ji, R., Ma, Y., 2020. Interactions between microplastics and organic pollutants: effects on toxicity, bioaccumulation, degradation, and transport. Sci. Total Environ. 748. https://doi.org/10.1016/j.scitotenv.2020.142427.

Yi, J., Ma, Y., Ruan, J., You, S., Ma, J., Yu, H., Zhao, J., Zhang, K., Yang, Q., Jin, L., Zeng, G., Sun, D., 2024. The invisible threat: assessing the reproductive and transgenerational impacts of micro- and nanoplastics on fish. In: Environment International, 183. Elsevier Ltd. https://doi.org/10.1016/j.envint.2024.108432.